

The influence of vibrational and translational motion on the reaction dynamics of $O(^1D) + H_2(^1\Sigma_g^+, \nu)$

Klaus Mikulecky and Karl-Heinz Gericke

*Institut für Physikalische und Theoretische Chemie der Johann Wolfgang Goethe-Universität,
Niederurseler Hang, 6000 Frankfurt am Main 50, Germany*

(Received 13 November 1991; accepted 5 February 1992)

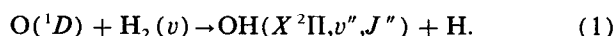
The OH product state distribution from the reaction $O(^1D) + H_2(\nu) \rightarrow OH(\nu'', J'', \Omega, \Lambda) + H$ was determined by laser-induced fluorescence (LIF) in the $\Delta\nu = -3$ band for $\nu'' = 3$ and 4 with resolution of the J'' , Ω , and Λ sublevels. The rotational state population distribution is inverted strongly in $\nu'' = 3$, weaker in $\nu'' = 4$. There is a higher propensity for production of OH in the $\Pi(A')$ Λ -sublevels. Vibrationally excited H_2 was used for a part of the experiments. Excitation was achieved by stimulated Raman pumping (SRP). The population ratio of the vibrational states was determined to be $P(\nu = 3)/P(\nu = 4) = 3.5$ for the reaction with $H_2(\nu = 0)$ and 3.0 when there is $H_2(\nu = 1)$ in the reaction chamber. Higher OH product states are populated than it would be expected from the mean available energy of the reaction. The translational energy of the reactants is transferred into OH rotation.

I. INTRODUCTION

Although the dynamics of chemical reactions has been subject of intense research for many years, there is still little experimental and theoretical evidence of the reaction dynamics of vibrationally excited species. Our knowledge on the influence of the translational energy on specific product states is also in the beginning. There have been a number of kinetic measurements, but state-to-state experiments have scarcely been performed yet. This may be due to the experimental difficulties of preparing a rotational-vibrational molecular state selectively. These difficulties have been overcome in recent years by the use of narrow bandwidth high power lasers which allow those selective excitations for performing state-to-state measurements by different techniques. Reactants that exhibit an infrared (IR) spectrum may be excited by tunable IR excitation, so as, e.g., HCl and HF, whose reactions with oxygen, alkaline metal, and alkaline earth metal atoms have been under investigation. A number of references on elastic, inelastic, and reactive atom-molecule collisions may be found in Refs. 1 and 2.

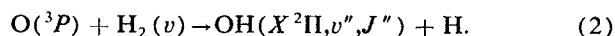
The use of homonuclear diatomic molecules as reactants causes considerably greater problems, for they do not exhibit an IR spectrum. For purely kinetic measurements it may be sufficient to excite those species to their higher vibrational levels thermally, but state-to-state experiments require a very high selectivity. This may be reached by stimulated Raman pumping (SRP), a convenient method which has been successfully used in the past.^{3,4} The only type of chemical reaction of vibrationally excited H_2 investigated in a state-to-state experiment up to this day is the hydrogen exchange reaction in its isotopic variant $D + H_2$.⁵ The use of vibrationally excited H_2 should exert large effects on the reaction dynamics. For reactions with an exit channel barrier there is an enhanced rate constant expected, and if there is no barrier at least the energetics of the reactions should change considerably. H_2 in the $\nu = 1$ state gives an addi-

tional energy of 4155 cm^{-1} to the reacting system which has to be partitioned to the various degrees of freedom of the reaction products. In this paper we would like to present our measurements on the reaction of oxygen atoms with vibrationally excited hydrogen molecules



(a) Reaction with $H_2(\nu = 0)$; $\Delta H_{298} = -181.6 \pm 1.4$ kJ/mol (Ref. 6). (b) Reaction with $H_2(\nu = 1)$; $\Delta H_{298} = -231.3$ kJ/mol. Furthermore, the influence of translational motion on the reaction dynamics is investigated by the observation of OH products in highly excited rovibrational states.

The reaction rate has been shown to be gas-kinetic, $\sim 1.1 \times 10^{-10} \text{ cm}^3 \text{ molecule}^{-1} \text{ s}^{-1}$.^{7-10,47} For several reasons, this reaction has been given quite considerable experimental¹¹⁻²⁴ and theoretical²⁵⁻³⁸ attention. The production of OH from this process plays an important role in the chemistry of the upper layers of the earth's atmosphere. In the laboratory it can be readily examined because the reactants, hydrogen and $O(^1D)$, are available or quite easy to produce, and the OH product can be analyzed spectroscopically by standard methods, such as laser-induced fluorescence (LIF) or IR chemiluminescence. Theoretical treatment can be done at moderate expense because of the relative low number of electrons involved. Similar arguments apply to the related ground state reaction³⁹



(a) Reaction with $H_2(\nu = 0)$; $\Delta H_{298} = 8.4$ kJ/mol, $k = 9 \times 10^{-18} \text{ cm}^3 \text{ molecule}^{-1} \text{ s}^{-1}$. (b) Reaction with $H_2(\nu = 1)$; $\Delta H_{298} = -41.4$ kJ/mol, $k = 10^{-14} \text{ cm}^3 \text{ molecule}^{-1} \text{ s}^{-1}$. However, this reaction is not accessible to state-to-state experiments performed in the usual laser pump and probe technique under single-collision conditions because of its quite low reaction rate constant

($\sim 9 \times 10^{-18}$ cm³ molecule⁻¹ s⁻¹),⁴⁹ which is enhanced by three orders of magnitude when vibrationally excited hydrogen reacts with the oxygen atoms.³⁹

In what concerns the reactions of O(¹D) with H₂ experimental effort has been directed to determining the rotational-vibrational and electronic fine structure distribution via LIF,^{12-14,17-19,22} chemical laser techniques,^{11,20} infrared chemiluminescence,^{16,21,23} and infrared spectroscopy.²⁴ The spatial distribution of the scattering products has been determined in a molecular beam experiment,¹⁵ and the influence of isotopic substitution was observed.^{17,19,24} Although some detailed information on the product state distribution is gained, it has not yet been determined unequivocally whether the energy partitioning is statistically or dynamicaly controlled.²³

Common to all experimental investigations is the observation of extremely high rotationally excited OH products in $v'' = 0, 1, 2, 3$. The peak of the OH population distribution is found regularly near to the limit of the available energy of the reaction. It should be mentioned that a highly inverted rotational distribution is also found in the reaction of O(¹D) with saturated hydrocarbons,⁴⁰ while the reaction of the metastable oxygen atom with water leads to a rotational OH product distribution which can be described by a temperature.^{41,42}

The population of the OH vibrational states is somehow more ambiguous. Measurements by infrared emission techniques yield inverted populations, in contrast to observations by the LIF technique, so that there are still questions unanswered. A quite important feature in what concerns the reaction mechanism is the population of the OH Λ -sublevels. These are due to the interaction of molecular rotation with orbit angular momentum and correspond to a certain symmetry maintained during the reactive collision. In all Λ state-specific investigations a clear propensity for the symmetric state, $\Pi(A')$, was observed, what corresponds to a Λ -state anti-inversion. The question of whether there is a Λ -state selectivity or not is important in order to clarify the way the reaction occurs, either via a collinear abstraction or a rectangular insertion process. The experimental evidence tends more to the insertion mechanism, because of the strong Λ -selectivity, which is not to be expected in an abstraction,

and because of the high rotational and weaker vibrational excitation. In the case of an abstraction mechanism one would expect contrary distributions, an inverted vibrational, and a considerably weaker rotational excitation.

In theory, emphasis was laid on the calculation of H₂O(\tilde{X}) potential energy surfaces using different methods, and treating the reactive scattering of the O(¹D)/H₂-system by trajectory calculations. Badenhoop *et al.* used a quantum mechanical method to calculate the energy distribution.³⁶ In general, even if this is an oversimplification compared to the great theoretical effort, one can summarize these studies in so far that the reaction mechanism expected by experimental evidence can be approved by calculations. There is a higher propensity for the rectangular insertion process (C_{2v} symmetry) than for the collinear abstraction ($C_{\infty v}$ symmetry) because of a higher entrance barrier for the latter. This entrance barrier might be overcome at high collision energies, so that in this case the calculations yield a higher vibrational excitation. Schinke and Lester²⁷ have examined the influence of H₂ vibrational excitation on the reaction dynamics. They found a totally changed OH product distribution, which is predicted to be highly inverted with its maximum at $v'' = 5$ or 6, depending on the collision energy. Because of the lack of an exit channel barrier this H₂ vibrational excitation has only a minor influence on the overall reaction rate. A synopsis of the experimental and theoretical results is shown in Tables I and II.

In this paper we intend to compare our experimental results with the calculations mentioned above. The use of vibrationally excited H₂ is promising to allow new insights into the dynamics of the O(¹D) + H₂ reaction, as well as it is of general interest with respect to the only poorly examined influence of vibrational excitation on reactive scattering. The observed rotational states of OH, $v'' = 3$ and 4, were chosen because of the Λ -state selectivity, the influence of the spin and the rotational distribution in $v'' = 4$ and its total population with respect to $v'' = 3$, which is not known yet by LIF experiments. Furthermore, these states are very near to the energy limit of the reaction, i.e., the OH vibrational excitation takes the greater part of the available energy. Therefore we can observe the OH product near to the energy threshold, where there are the largest influences of the H₂

TABLE I. Measured OH product vibrational populations. LIF = laser induced fluorescence; IR-CL = infrared chemiluminescence; Chem. L. = chemical laser.

Method	Populations					Ref.	Remarks
	$v = 0$	$v = 1$	$v = 2$	$v = 3$	$v = 4$		
LIF	1.0	1.0				13	266 nm photolysis
IR-CL		0.26	0.29	0.28	0.16	16	248 nm photolysis
LIF	1.0	1.04				19	248 nm photolysis
Chem. L.	1.0	0.69	0.63	0.51	<0.36	20	flashlamp photolysis
IR-CL		0.29	0.32	0.25	0.13	21	248 nm photolysis
LIF			1.0	0.39		22	248 nm photolysis
LIF				1.0	0.293	This work	266 nm photolysis

TABLE II. Theoretically calculated vibrational populations of the OH product. QCT = quasiclassical trajectory calculation; DIM = diatomics in molecules; QRS = quantum reactive scattering; MC = Monte Carlo simulation.

Method	Populations						Ref.	E (kJ/mol)
	$\nu = 0$	$\nu = 1$	$\nu = 2$	$\nu = 3$	$\nu = 4$	$\nu = 5$		
QCT	0.244	0.223	0.217	0.156	0.097	0.063	27	2.1
VB-DIM	4.6	3.3	3.2	0.4	0.4	...	29	8.4
QCT	273	343	331	419	376	209	30	21
QCT	1	0.73	0.98	0.67	0.07	0	31	3.3
MC	1	0.81	0.58	0.29	0.01	...	34	...
QCT	0.324	0.318	0.204	0.127	0.022	0	35	2.1
QRS	0.22	0.1	0.15	0.18	0.03	0	36	21
MC	0.22	0.18	0.19	0.16	0.15	0.09	37	2.1
DIM	1	0.87	0.55	0.3	0.15	0	38	8
QCT	1	0.87	0.58	0.37	0.13	0	54	8

vibrational excitation on the OH rotational-vibrational distribution to be expected. Further, the influences from the translational excitation of the reactants on the OH product state distribution are easier to observe under threshold conditions.

II. EXPERIMENT

Electronically excited oxygen atoms in the 1D state were generated in a pulsed laser photolysis of ozone. Ozone was prepared in a silent discharge in O_2 (99.95% purity) and trapped on cooled silica gel (170 K, ethanol slush) in a U-tube. To remove oxygen, the U-tube was evacuated shortly, and the ozone and remainders of O_2 were condensed afterwards into a liquid nitrogen cooled trap. From there the rest of O_2 could be removed by evacuating. Prior to the experiments the ozone had to be expanded into a 6 l glass flask, at a pressure below 100 Torr. It was introduced into the reaction chamber through stainless steel pipes and valves. Hydrogen (purity 99.9999%) was used without further purification. To avoid any risk of detonations, the reactants were mixed in the reaction chamber, and not prior to it. The partial pressures of the reactants were 13 Pa each, controlled by a MKS Baratron capacitance gauge. The reaction chamber was evacuated by an oil diffusion pump, reaching a base pressure of $\sim 10^{-2}$ Pa. The experimental setup is shown in Fig. 1.

The reaction was initiated by firing a frequency quadrupled Nd:YAG laser (Quanta-Ray DCR 1A) into the cell, whose focused output photolyzes ozone to $O(^1D)$ and O_2 ,⁴³ the former of which reacts rapidly with hydrogen. It is advantageous to enter the laser radiation through MgF_2 rather than suprasil windows, because the high power density of the laser (pulse energy = 40 mJ, pulse width = 5 ns) is able to damage suprasil windows by two-photon effects.

For experiments with vibrationally excited hydrogen the frequency doubled output of a Nd:YAG laser (Spectron SL2Q) was focused through a H_2 pressure Raman shifter [$P(H_2) = 10$ bar] into the reaction chamber, parallel to the photolysis pulse and ~ 50 ns prior to it. This time delay is due to the difference in the response times of the Q switches

of the YAG lasers, which were triggered simultaneously. The Raman shifter generated the Stokes and anti-Stokes radiation of hydrogen, which, if focused into the reaction chamber, excited the ($\nu = 1 \leftarrow \nu = 0$) transition of H_2 .³⁻⁵ In some preceding experiments we observed that our Raman shifter produces high-order anti-Stokes radiation which reaches the Hartley band wavelength of O_3 , i.e., produces $O(^1D)$. To achieve higher selectivity in the photolysis we decided to cut off the shorter wavelengths (below 350 nm) by a filter. In the H_2 excitation there are, due to the selection rules for homonuclear diatomics only the $\Delta J = 0, \pm 2$ transitions accessible (O, Q, S branches).⁴⁴ Roughly 20% of the H_2 are vibrationally excited.⁵ Vibrational relaxation of H_2 needs not to be taken into account, for the spontaneous transition to the vibrational ground state is dipole-forbidden and we worked under single-collision conditions.

Probing the OH product was done with an excimer pumped dye laser, Lambda Physik LPX 100 and FL 2002 E. The dye laser was operated with Coumarin 2 at a pulse ener-

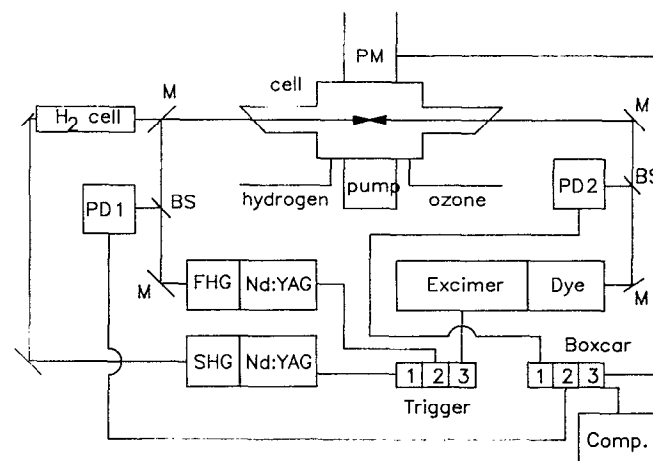


FIG. 1. Schematic drawing of the experimental setup.

gy of ~6 mJ. Linear dependence of the OH LIF signal from the probe laser power was checked by decreasing the power by filters of known transmission. A continuous nuisance to the experiment was the very low stability of the dye, which had to be replaced after two days of operation. The dye laser beam counterpropagated the beams of the 266 nm photolysis and the Raman shifter output collinearly. It was fired with 200 ns delay after the initiating photolysis pulse. We excited the (*A* ²Σ, *v*' = 0, *J*') ← (*X* ²Π, *v*" = 3, *J*"') and (*A* ²Σ, *v*' = 1, *J*') ← (*X* ²Π, *v*" = 4, *J*"') transitions of OH in order to compare the relative populations in *v*" = 3 and 4. Direct excitation of the diagonal Δ*v* = 0 transitions is not possible for OH because it undergoes strong predissociation in the *A*-state beginning with *v*" = 2.⁴⁵

The measurements were carried out at a pulse repetition rate of 10 Hz. Repetition rate and delay times were controlled by a delay generator. The powers of the photolysis and probe lasers were recorded by photoelectric detectors (Hamamatsu) in order to normalize the LIF signal. The LIF signal itself was observed with a photomultiplier (Valvo). OH LIF spectra were recorded from 440 to 460 nm, once for the reaction with ground state and once for the reaction with vibrationally excited H₂.

Additionally, we would like to mention that we tried another way of O(¹D) generation, besides the conventional ozone photolysis. The two-photon dissociation of NO₂, first step excitation with 532 nm, second step dissociation of the excited molecule with 355 nm, yields O(¹D) as well.⁴³ The advantage of this method is that the ozone preparation becomes unnecessary, NO₂ is readily available, but this showed to be outweighed by the disadvantages. The 532 nm-excited NO₂ fluoresces strongly in the visible and near-ultraviolet (UV). This disturbs measurements of weakly populated vibrational OH states from the examined reaction to an extent that we decided to use ozone again. Besides, NO₂ is quite reactive and causes corrosion on the gas manifold pipes and valves so that its use as a O(¹D) precursor is not recommendable.

III. RESULTS

The line intensities *I* derived from the OH LIF spectra were converted into populations *P* by normalizing them with respect to the transition probabilities. These transition probabilities for the process (*A* ²Σ; *v*' = 0, 1; *J*') ← (*X* ²Π; *v*" = 3, 4; *J*"') were taken as the product of the Franck–Condon factor for the vibrational transition *q*_{vib} and the Hönl–London factor for the rotational transition *H*_{rot}. The Franck–Condon factors,⁵³ OH levels⁴⁴ and transition probabilities⁴⁵ were taken from the literature,

$$P \sim \frac{I}{(2J + 1)q_{\text{vib}}H_{\text{rot}}} \quad (3)$$

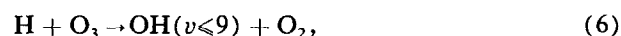
According to the difference in spontaneous emission probability (Einstein *A* coefficient) between transitions starting from *v*' = 1 and *v*' = 0 to *v*" = 1 and *v*" = 0 it was necessary to enhance the populations derived for *v*" = 4 by 25%, because the interference filter attached to the photomultiplier optics rejected the wavelengths of ~280 nm related to the emission process OH(*A* ²Σ *v*' = 1)

→ (*X* ²Π, *v*" = 0). This transition takes ~25% of the total OH (*A*) population to the electronic ground state.⁴⁸

Further reactions of the primary reaction products OH and H need not to be taken into account. Possible reactions are



and



with collisional relaxation



Reactions (4) and (5) are of no further importance, for they are very slow ($k \leq 7 \times 10^{-14} \text{ cm}^3 \text{ molecule}^{-1} \text{ s}^{-1}$),⁴⁹ and even if they should occur, they could not disturb the measurements because they just remove OH from the area of detection, i.e., just lower the signal intensity but do not produce OH in other rotational–vibrational states. Reaction (6) is much faster, $k = 2.8 \times 10^{-11} \text{ cm}^3 \text{ molecule}^{-1} \text{ s}^{-1}$.⁴⁹ However, for a collisional relaxation of OH at an assumed rate constant of $10^{-10} \text{ cm}^3 \text{ molecule}^{-1} \text{ s}^{-1} < 15\%$ of the OH molecules formed in reaction (1) will relax prior to detection. Thus, the influence of the secondary reactions (6) and (7) on the OH product state distribution is negligible. Cleveland *et al.*²² have outlined that there is no necessity to correct the LIF intensities for the differences in the fluorescence quenching cross section between the rotational levels of OH (*A* ²Σ).

A. Rotational distribution

The rotational distributions in *v*" = 3 and 4 are shown in Fig. 2. A distinction is made between reactions involving H₂ (*v* = 1) and those which do not. The energy limit for the rotational–vibrational excitation, as can be calculated from energy conservation, is 15 980 cm⁻¹ for the O(¹D) + H₂ (*v* = 0) reaction and 20 130 cm⁻¹ for the O(¹D) + H₂ (*v* = 1) reaction. In the Boltzmann plot for the vibrational ground state reaction the limit is indicated by a line. *E*_{av} is obtained by adding the exothermicity of the reaction, Δ*H*, the internal energy of H₂, *E*_{int} = *E*_{rot} + *E*_{vib} and the collision energy between thermal H₂ and O(¹D) from the ozone photolysis. The internal energy of H₂ is purely rotational. The first vibrational level of H₂ is not excited at room temperature because of its very high energy above the ground state. The rotational distribution was assumed to be of Boltzmann-type, and the mean rotational energy was calculated to be *E*_{rot} = 1.92 kJ mol⁻¹.

The collision energy between H₂ and O(¹D) has to be determined in the center-of-mass frame⁴²

$$E_{\text{trans}}(\text{O}, \text{H}_2) = \frac{1}{2} \mu(\text{O}, \text{H}_2) [3RT/M(\text{H}_2) + 3RT/M(\text{O}_3) + 2E_{\text{trans}}(\text{O}, \text{O}_2) \mu(\text{O}, \text{O}_2)/M^2(\text{O})]. \quad (8)$$

The translational center-of-mass energy of O(¹D) and O₂ from the ozone photolysis at 266 nm, *E*_{trans}(O, O₂), was determined by Sparks *et al.*⁵⁰

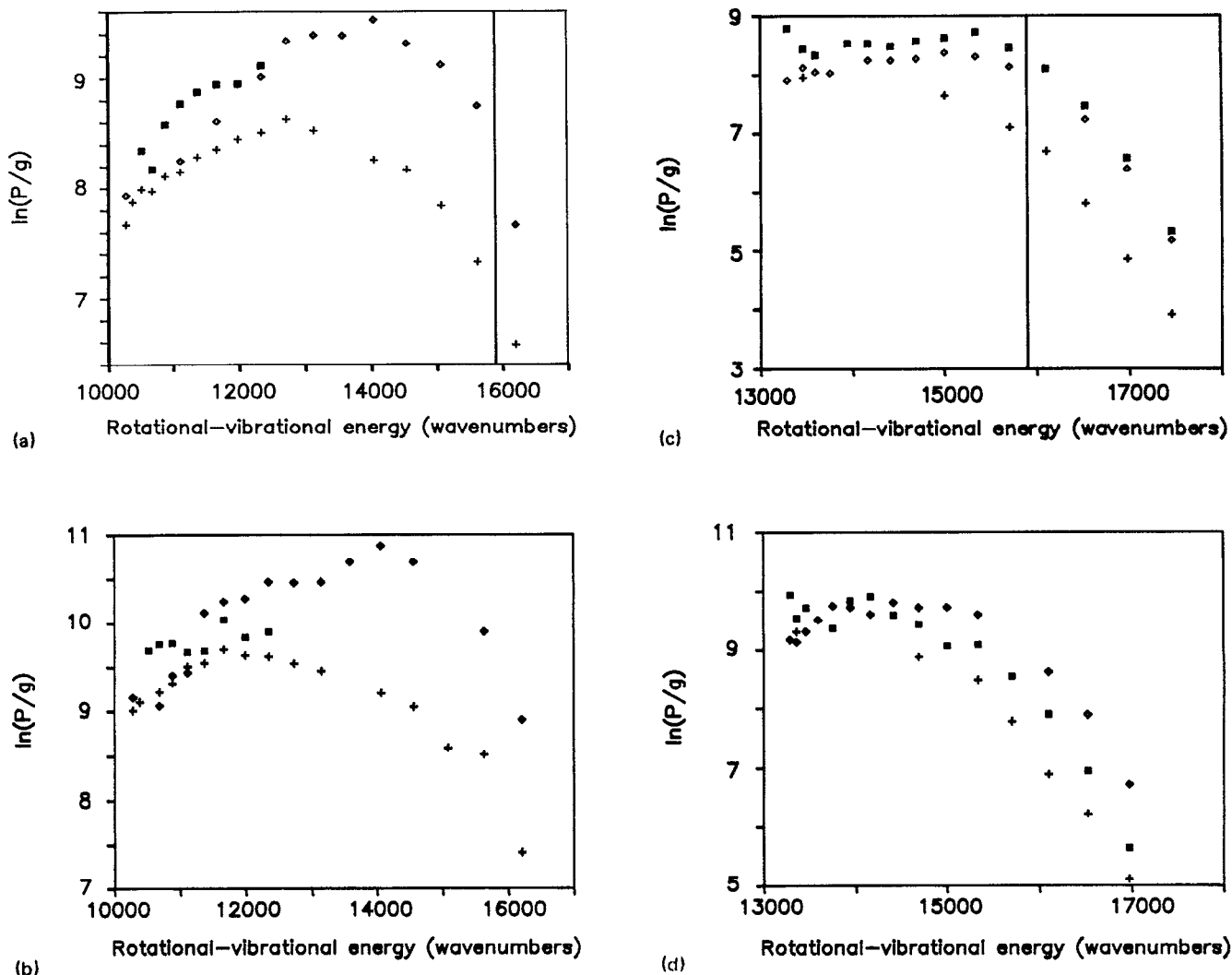


FIG. 2. Boltzmann plot of the rotational distribution in $v'' = 3$ and 4 , where P represents the population and g is the degeneracy. Symbols for the different branches are R , \blacksquare ; Q , $+$; P , \blacklozenge . (a) $OH(v'' = 3)$, $H_2(v = 0)$; (b) $OH(v'' = 3)$, $H_2(v = 0, 1)$; (c) $OH(v'' = 4)$, $H_2(v = 0)$; (d) $OH(v'' = 4)$, $H_2(v = 0, 1)$. The thermochemical limit for the OH rotational energy is indicated by a vertical line.

The distributions are clearly inverted in $v'' = 3$, with a peak near to the energetic limit for the P lines, the Q distribution is flatter. In $v'' = 4$ there is still an inverted population distribution in the P branch, but not as strong as in $v'' = 3$. The Q branch of the spectrum does not exhibit a peak any more, it has become decreasing monotonically. The rotational distributions emerging from the reaction with vibrationally excited hydrogen do not differ strongly from those with ground state H_2 . Variations in relative population numbers are less than a few percent (Fig. 3).

B. Vibrational distribution

The vibrational distribution emerging from the $O(^1D) + H_2$ reaction is a critical feature in the experiments, as was already outlined in the Introduction. This can be explained by the specific difficulties in the determination of $P(v)$. The rotational distribution of the OH product is not thermal, but inverted. So there is no simple statistical method, like extrapolating the rotational distribution to $E_{rot} = 0$, to obtain rel-

ative population numbers for comparison. It is necessary to add the population of single rotational states. Summation over all rotational states requires that all the rotational lines of the spectrum are observable, i.e., that they do not overlap, which is not the case for the $\Delta v = -3$ band of the OH spectrum. The missing lines have to be obtained by interpolation. Another problem may be the predissociation of the higher rotational-vibrational levels of the $OH(A^2\Sigma)$ state. In the case of this reaction, where highly rotationally excited OH is generated, the predissociation rate of $OH(A)$ has to be taken into account for evaluating a LIF spectrum, when levels higher than $N'' = 25$ in $v'' = 0$ and $N'' = 16$ in $v'' = 1$ are observed. Very high rotational states of OH become totally inaccessible by LIF in the $(\tilde{A} \leftarrow \tilde{X})$ band, for predissociation reduces their radiative lifetime to the picosecond regime. This is especially a problem when investigating the low vibrational levels of the OH product. In the present experiment the influence of predissociation is negligible because the highest populated state in $v'' = 3$ is $N'' = 19$ and in $v'' = 4$ it is $N'' = 15$.

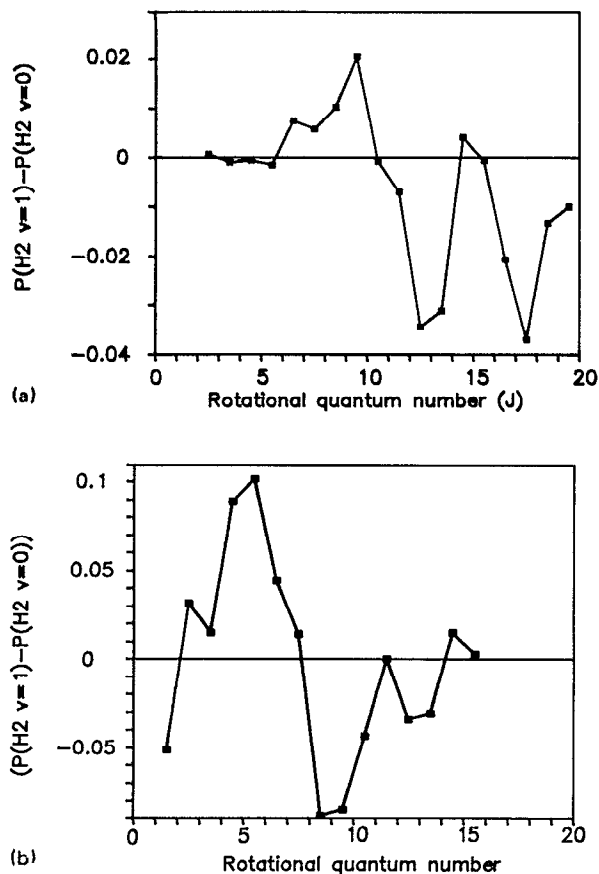


FIG. 3. Differences between the populations of the rotational levels of OH with and without vibrationally excited H₂. The populations are normalized to 1. (a) OH($v'' = 3$); (b) OH($v'' = 4$).

The determination of vibrational populations is also quite sensitive to the vibrational transition probabilities. These Franck–Condon factors are reported quite different in the literature, as was mentioned more detailed in a previous paper.⁵³

By comparing the sums of population numbers we obtained a population ratio $P(v'' = 3)/P(v'' = 4)$ of 3.5 for the reaction of vibrational ground state H₂ and of 3.0 for vibrationally excited H₂. This means that the population of $v'' = 4$ compared to that of $v'' = 3$ is $\sim 15\%$ higher when vibrationally excited hydrogen is used as reactant. This is a considerable amount for it has to be taken into account that only 20% of the hydrogen were vibrationally excited. Thus, the calculated increase of OH vibration is more than 70% with H₂ ($v = 1$) being the only reaction partner of O(¹D). However, it should be mentioned that the determination of the vibrational population is subject to an error of up to 10%, and the increase of OH vibration has to be taken more qualitatively than as an exact number. Nevertheless, the formation of OH ($v = 4$) is clearly preferred, when vibrationally excited H₂ educt molecules are involved in the reactive collision process.

C. Electronic fine structure distribution

The OH molecule exhibits two types of electronic fine structure, the spin–orbit and the Λ splitting. The former re-

sults from interaction of the spin of the unpaired electron with the orbital angular momentum, and the latter emerges from coupling of orbital angular momentum with the nuclear rotation. We found no evidence for spin selectivity in the reaction of O(¹D) with H₂ (¹ Σ_g^+). In general, for reactions of particles in singlet states this is not to be expected either.

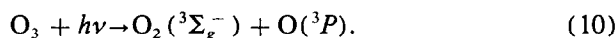
A totally different behavior is observed for the Λ sublevels. Their population can be determined by calculating the difference of population exhibited by the P , R , and Q branches of the spectrum. The P , R lines probe the symmetric $\Pi(A')$ Λ component, the Q lines probe the antisymmetric $\Pi(A'')$ Λ component. In the ² $\Pi_{3/2}$ system the $\Pi(A'')$ sublevels are always higher in energy than the $\Pi(A')$ components, in the ² $\Pi_{1/2}$ system this is the case for $N > 4$.⁴² The population ratio is calculated by

$$f_\Lambda = \frac{P[\Pi(A'')] - P[\Pi(A')]}{P[\Pi(A'')] + P[\Pi(A')]} \quad (9)$$

A negative value of f_Λ means that the $\Pi(A')$ component is the higher populated one, i.e., the system exhibits a Λ doublet anti-inversion, which is observed in the present experiment. This strong preponderance of the lower Λ component is shown in Fig. 4. The Λ selectivity of the reaction is an important feature to elucidate the mechanism of the reactive collision.

D. The influence of the O(³P)+H₂ reaction

The photolysis of ozone at 266 nm generates not only O(¹D) atoms, but also O(³P) atoms with a quantum yield of $\sim 10\%$,⁴⁹



As might be expected, the kinetic center-of-mass energy of O₂ and O(³P) is considerably higher than in the case of the O(¹D) production. The high velocity of the O(³P) atoms could be sufficient to overcome the reaction barrier for the

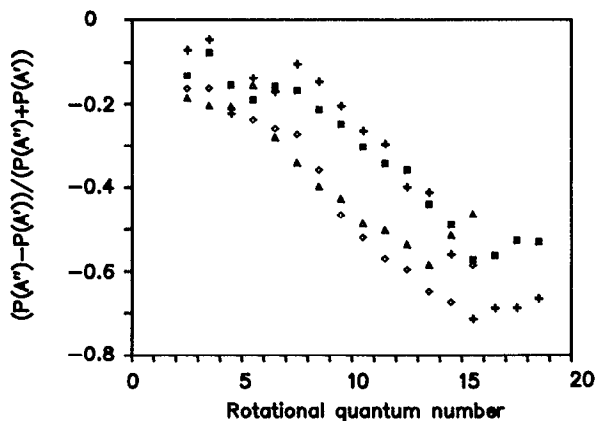


FIG. 4. A doublet population inversion. $P(A')$ represents the population of the symmetric and $P(A'')$ is the population of the antisymmetric Λ sublevel. ■, OH($v = 3$), H₂($v = 0$); +, OH($v = 3$), H₂($v = 0$) + H₂($v = 1$); ◇, OH($v = 4$), H₂($v = 0$); ▲, OH($v = 4$), H₂($v = 0$) + H₂($v = 1$).

O(³P) + H₂ reaction. The kinetic center-of-mass energy for an O(³P)-H₂ collision is $E_t = 28.3 \text{ kJ mol}^{-1}$. This is a result of Eq. (8), where a translational energy of $E_t = 334.4 \text{ kJ mol}^{-1}$ is used.⁴⁹ Thus, the collision velocity of O(³P) and H₂ is calculated to be $v(\text{O}, \text{H}_2) = 5640 \text{ ms}^{-1}$. For thermally distributed O(³P) and H₂ this velocity is 2170 ms^{-1} . From the temperature dependence of the reaction rate of O(³P) + H₂ (Ref. 47) the rate constant for the mentioned collisional velocity can be calculated to be $k = 2.5 \times 10^{-12} \text{ cm}^3 \text{ molecule}^{-1} \text{ s}^{-1}$. Thus, it is about two orders of magnitude smaller than the (nearly temperature independent) rate constant of the O(¹D) reaction. For a fixed pump-probe delay the amount of OH produced by the O(³P) reaction is given by

$$f[\text{O}(\text{}^3\text{P})] = \frac{k[\text{O}(\text{}^3\text{P})]}{k[\text{O}(\text{}^1\text{D})]} \cdot \phi[\text{O}(\text{}^3\text{P})] = 6.8 \times 10^{-3}.$$

This fraction of OH products from the reactive collisions between translationally hot O(³P) and H₂ of < 1% of the amount produced by O(¹D) is neglected for the considerations in this paper.

We have made an attempt to observe OH from the ground state oxygen plus hydrogen reaction,² but without success. The O(³P) was generated by a 355 nm laser pulse from a frequency tripled Nd:YAG laser by photolysis of NO₂. As was already outlined in the Introduction, the reaction rate constant of Eq. (2) is too small to produce enough OH in the time of a few hundred nanoseconds which are necessary to perform a pump-and-probe experiment under single collision conditions.

IV. DISCUSSION

An amazing feature is the very high rotational excitation even in $v'' = 3$ and 4 which exceeds the mean available energy for the products by $\sim 1000 \text{ cm}^{-1}$. The implication by conservation of energy and angular momentum on the reaction process will be discussed in the following.

Angular momentum conservation leads to the equation

$$\begin{aligned} J_{\text{tot}} &= \mathbf{J}[\text{O}(\text{}^1\text{D})] + \mathbf{J}(\text{H}_2) + \mathbf{L}(\text{O}, \text{H}_2) \\ &= \mathbf{J}(\text{OH}) + \mathbf{J}(\text{H}) + \mathbf{L}(\text{OH}, \text{H}), \end{aligned} \quad (11)$$

where L denotes the orbital angular momentum of the colliding species or the reaction products. J represents the angular momentum of the respective particles. It is $2\hbar$ for O(¹D) and $1/2 \hbar$ for H. $J(\text{H}_2)$ was assumed to equal $1\hbar$, because in the thermal equilibrium more than two thirds of the H₂ is in the $J = 1$ rotational state. Since the observed OH products are highly rotationally excited, the orbital angular momentum is an important quantity to guarantee conservation of the total angular momentum J_{tot} .

A. Orbital angular momentum and impact parameter

L is linked to the impact parameter b by

$$L = \mu v b. \quad (12)$$

(All symbols mean absolute values, not vectors, unless denoted otherwise.) From Eq. (14) and the rate constant k at a

velocity independent cross section σ_0 ,

$$k = v\sigma_0 = v\pi b^2 \quad (13)$$

follows the maximum value of the impact parameter

$$b = (k/\pi v)^{1/2}. \quad (14)$$

For the mean center-of-mass velocity of the educts in a thermal equilibrium this gives $b_e = 110 \text{ pm}$ which is larger than the H-H bond length of 74.2 pm . The orbital angular momentum is calculated to be $L(\text{O}, \text{H}_2) \simeq 9\hbar$ and a maximum total rotation $J_{\text{tot},e}$ of $\sim 12\hbar$ has to be conserved, where mean values of v and $J(\text{H}_2)$ have been used.

For maximum coupling of the educt angular momenta and minimum coupling of the product angular momenta (in order to consider the extremely high OH rotation) it follows from Eq. (11),

$$L_e + 3\hbar \geq J(\text{OH}) - J(\text{H}) - L_p$$

or

$$L_p \geq J(\text{OH}) - L_e - 3.5\hbar,$$

by substituting L from Eq. (12),

$$\mu_p v_p b_p \geq J(\text{OH}) - \mu_e v_e b_e - 3.5\hbar. \quad (15)$$

The impact parameter for the products, b_p , has to be determined. This is more complicated, for we did not measure the fragment velocity of the OH product. However, energy conservation requires

$$\Delta E + \frac{1}{2}\mu_e v_e^2 = \frac{1}{2}\mu_p v_p^2 + E_{\text{int}}(\text{OH}) \quad (16)$$

with

$$\Delta E = \Delta H^0 + E_{\text{int}}(\text{H}_2).$$

Substituting Eq. (16) into Eq. (15) leads to

$$b_p \geq \frac{J(\text{OH}) - \mu_e v_e b_e - 3.5\hbar}{\{\mu_p [2 \cdot \Delta E + \mu_e v_e^2 - 2 \cdot E_{\text{int}}(\text{OH})]\}^{0.5}}. \quad (17)$$

From Eq. (17) we can determine a lower bound for the product impact parameter b_p . Extremely large values of b_p are unlikely, what implies that the chance of a reactive collision is lower at that educt velocity v_e . In that case the reaction is limited by the constraint of conservation of angular momentum. A plot of b_p and v_p as a function of the relative educt velocity v_e is shown in Fig. 5, where the mean value of ΔE is used. The negative lower limit for b_p means that conservation of angular momentum is no restriction for reactive encounters. The reaction is always possible when there is enough energy to produce a specific OH rotational state. The conservation of angular momentum can always be fulfilled by the orbital angular momentum of the reaction products. The limiting factor is the available energy.

B. Influence of the reactant translational excitation on the products

The very high rotational excitation exceeds the exothermicity of the reaction by $\sim 1000 \text{ cm}^{-1}$. This effect can only be explained by the relative velocity of the reactants, namely of H₂. The value of $15\,980 \text{ cm}^{-1}$ for the average energy limit is calculated from the average kinetic energies of H₂ and O₃ in a thermal equilibrium, which in the case of O(¹D) the average kinetic energy as produced in the the ozone photoly-

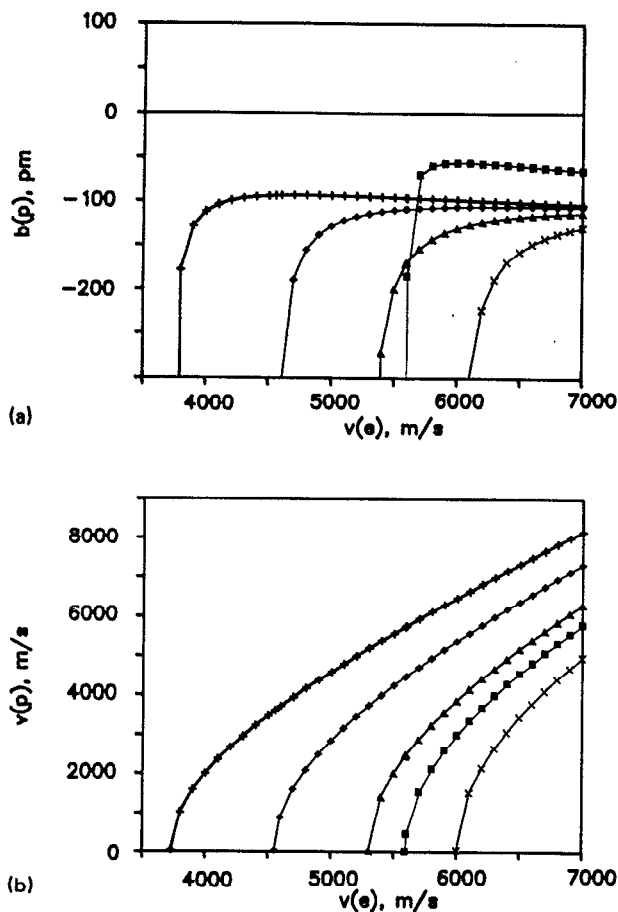


FIG. 5. (a) The impact parameter of the reaction products, b_p , and (b) their center-of-mass velocity, v_p , as a function of the reagent's relative velocity, v_r , and of the rotational levels of the OH product. ■, $v'' = 3$, $J'' = 19$; +, $v'' = 4$, $J'' = 12$; ◆, $v'' = 4$, $J'' = 13$; ▲, $v'' = 4$, $J'' = 14$; ×, $v'' = 4$, $J'' = 15$.

sis was taken. From Eq. (8) it can be seen easily that the velocity of ozone has only a minor effect on the total energy of the reaction, due to the high mass of O relative to H₂. The dominant kinetic energy contribution to the available energy is therefore given by the H₂ molecule, and, to a considerably smaller amount, by the O(¹D) atom. To get a quantitative estimate of this influence we have to calculate the number of H₂ molecules that exceed the mean thermal equilibrium velocity or kinetic energy.

The fraction of molecules $N(E_i)/N$ that exceed a given translational energy E_i in a Maxwell-Boltzmann distribution can be calculated by

$$N(E_i)/N = 2 \cdot (E_i/\pi kT)^{0.5} \cdot \exp(-E_i/kT) + 1 - \operatorname{erf}[(E_i/kT)^{0.5}], \quad (18)$$

where erf represents the error function.⁵²

A comparison between the populations of the OH in rotational-vibrational states that exceed the available energy of the reaction and the fraction of the H₂ molecules that have sufficient kinetic energy to allow the generation of these OH product states is given in Table III. The amount of high energy-OH (rotation) is always smaller than the amount of

TABLE III. The fraction of the total amount of H₂, $N(\text{H}_2)$, that has sufficient translational energy to produce the respective rotational-vibrational state of OH, $\text{OH}(v'', J'')$. The ratios between the total populations of $\text{OH}(v'', J'')$ and the total amount of translationally excited H₂ is always smaller than 1. However, a significant amount of translational energy of the educts is found as rotational energy of the OH product.

$v''(\text{OH})$	$J''(\text{OH})$	$N(\text{H}_2)$	$P(\text{OH}, v'', J'')/N(\text{H}_2)$	
			$\Pi(A'')$	$\Pi(A')$
3	19.5	0.14	0.013	0.0166
4	12.5	0.23	0.006	0.01
4	13.5	0.03	0.02	0.045
4	14.5	0.005	0.05	0.12
4	15.5	0.0003	0.35	0.64

high-energy H₂ (translation), so the production of the former may be explained by the Boltzmann distribution of H₂. The translational motion of the educts is transferred into rotation of the product molecule.

C. Product energy distribution

The H-O-H potential energy surface and the geometry of the reactive collision have to be related to the observed OH product energy state distribution from the O(¹D) + H₂ reaction and the influence of H₂ vibrational and translational motion. The H-O-H potential energy surface is dominated by a deep minimum at the ground state configuration of H₂O and an increase of energy in the exit channel of the reaction. Therefore a statistical product energy state distribution might be expected, because the reaction products need a longer time to separate from each other as if the surface were more flat. A longer duration of the reactive collision, i.e., a longer lifetime of the collision complex, allows internal energy redistribution.

A strong inversion of the OH product rotational states is observed experimentally. Normally this would be regarded as a sign of nonstatistical influences, but calculations show that the inverted rotational distributions are an outcome of angular momentum restrictions for the OH product with respect to the H-O-H collision complex. They occur even if a statistical partition of energy to the degrees of freedom is assumed.³⁴

The question of whether the abstraction or the insertion mechanism plays the most important role for the O(¹D) + H₂ reaction can be answered most decisively by examining the Λ -state distribution in the high vibrational states. The Λ -state selectivity in this reaction is an outcome of the well-known principle of symmetry conservation in chemical reactions. The reaction of two species which are symmetric with respect to the point group valid for the geometry of the reagent's approach produces two species which are symmetric in this meaning as well. Occasionally a dual reaction mechanism is proposed.²³ The reactive collisions should occur partly in C_{2v} geometry (insertion), producing high rotationally, low vibrationally and strong Λ -state selective populated OH, and partly in $C_{\infty v}$ geometry

(abstraction) with opposite properties. This could even lead to a bimodal vibrational distribution of the OH product. We conclude from our results that this is not the case. If an abstraction mechanism would be responsible for the production of high vibrationally excited OH then one has to expect a very low Λ -state selectivity for $OH(v'' = 4)$, combined with a low rotational excitation. This is not the case. There is, like for the other vibrational states, a strong propensity for the production of OH in the $\Pi(A')$ state, i.e., an anti-inversion of the Λ doublets. Therefore we conclude that the reaction of $O(^1D)$ with H_2 occurs via an insertion mechanism.

In a pictorial view, the oxygen atom inserts in the H_2 bond in order to "reach" the stable H_2O well. This transition state can be regarded as a highly excited bending mode of H_2O . When energy is transferred from the bending mode to the asymmetrical stretch, the collision complex dissociates leading to highly rotating OH products. An increase in the $O + H_2$ collision energy corresponds in this picture to an excitation of an even higher bending vibration. In that case, the energy will be transferred faster to the asymmetrical stretch mode and less time is left for an energy randomization. The reaction will be more direct and this very energy-rich H_2O molecule "lives" fewer vibrational periods than the collision complex formed by translationally slow educts. As a consequence, we predict a forward-backward asymmetry in an angle-resolved scattering experiment when OH products in high rotational states are generated at high collision energies.

A crucial feature is the OH vibrational state distribution, for reasons mentioned in previous sections and for comparison with theoretical calculations. From the papers quoted above where vibrational state distributions were calculated values for $P(v = 4)/P(v = 3)$ between 1.0 and 0.1 can be extracted. We have to concede that the presumed collision energies do not match exactly the conditions of our experiment, but the differences are large.

Schinke and Lester²⁷ calculated in addition to the OH vibrational state distribution for the H_2 reactant in $v = 0$, that one for H_2 in $v = 1$. They predict a change in the population ratio from $P(v = 4)/P(v = 3) = 0.63$ to 1.35 when vibrationally excited H_2 is used for the reaction. Berg *et al.* obtained in a semiclassical trajectory study a ratio of $P(v = 4)/P(v = 3) = 0.34$ for $H_2(v = 0) + O(^1D)$ which increased by almost a factor of 3 when hydrogen was excited to the $v = 4$ state.⁵⁴ Our experimental results show the same tendency. We observed a $\sim 15\%$ higher population in $OH(v'' = 4)$ when vibrationally excited hydrogen was used in the reaction. Repeatedly, it should be mentioned that the SRP efficiency for the conversion of $H_2(v = 0)$ to $v = 1$ is not higher than 20%. Thus, the population ratio $P(v = 4)/P(v = 3)$ should increase by 70% when H_2 is vibrationally excited. The H_2 vibrational excitation does not show a strong effect on the OH product rotational state distribution (Fig. 4). However, the general trend seems to be a slight decrease of the OH rotational excitation. Low rotational, and high vibrational excitation of the OH product is expected for an abstraction path but not for an insertion reaction. Thus, there seems to be a change in the reaction dynamics when vibrationally excited H_2 is used as reactant.

Perhaps "head-on" collisions become more favorite and contribute additionally to the OH product rotations. This speculation is supported by the trajectory study of Berg *et al.*,⁵⁴ where the only energetic effect for the $H_2(v = 0) + O(^1D)$ reaction is a reorientation of the reaction system toward a C_{2v} geometry. However, the $H_2(v = 4) + O(^1D)$ surface is found to be attractive for all orientations and the attraction extends further for the collinear than for the perpendicular, C_{2v} , configuration.

In summary, the reaction of $O(^1D)$ with $H_2(v = 0)$ is governed by an insertion process. The collision energy is significantly transferred into product rotation, and, thus, the product rotation becomes more and more dynamically controlled. Excitation of the H_2 vibration causes a probability for the generation of vibrationally excited OH product molecules.

ACKNOWLEDGMENTS

This work was performed as part of a program of the Deutsche Forschungsgemeinschaft (DFG). Financial support is gratefully acknowledged. We thank Professor Dr. F. J. Comes for helpful discussions and material support.

- ¹ H. G. Rubahn and K. Bergmann, *Annu. Rev. Phys. Chem.* **41**, 735 (1990).
- ² I. W. M. Smith, in *Bimolecular Collisions*, edited by M. N. R. Ashfold and J. E. Baggott (The Royal Society of Chemistry, London, 1989).
- ³ W. Meier, G. Ahlers, and H. Zacharias, *J. Chem. Phys.* **85**, 2599 (1986).
- ⁴ Y. Zhu, Y. Huang, S. Arepalli, and R. J. Gordon, *J. Appl. Phys.* **67**, 604 (1990).
- ⁵ D. A. V. Kliner and R. N. Zare, *J. Chem. Phys.* **92**, 2107 (1990).
- ⁶ JANAF Thermochemical Tables, *Natl. Stand. Ref. Data Ser. Natl. Bur. Stand.* **37** (1979).
- ⁷ J. A. Davidson, C. M. Sadowski, H. I. Schiff, G. E. Streit, C. J. Howard, D. A. Jennings, and A. L. Schmeltekopf, *J. Chem. Phys.* **64**, 57 (1976).
- ⁸ R. F. Heidner and D. Husain, *Int. J. Chem. Kinet.* **5**, 819 (1973).
- ⁹ L. J. Stief, W. A. Payne, and R. B. Klemm, *J. Chem. Phys.* **62**, 4000 (1975).
- ¹⁰ R. A. Young, G. Black, and T. G. Slanger, *J. Chem. Phys.* **49**, 475 (1986).
- ¹¹ G. D. Downey, D. W. Robinson, and J. H. Smith, *J. Chem. Phys.* **66**, 1685 (1977).
- ¹² G. K. Smith, J. E. Butler, and M. C. Lin, *Chem. Phys. Lett.* **65**, 115 (1979).
- ¹³ G. K. Smith and J. E. Butler, *J. Chem. Phys.* **73**, 2243 (1980).
- ¹⁴ A. C. Luntz, R. Schinke, W. A. Lester, and H. H. Günthard, *J. Chem. Phys.* **70**, 5908 (1979).
- ¹⁵ R. J. Buss, P. Casavecchia, T. Hirooka, S. J. Sibener, and Y. T. Lee, *Chem. Phys. Lett.* **82**, 386 (1981).
- ¹⁶ J. E. Butler, R. G. MacDonald, D. J. Donaldson, and J. J. Sloan, *Chem. Phys. Lett.* **95**, 183 (1983).
- ¹⁷ K. Tsukiyama, B. Katz, and R. Bersohn, *J. Chem. Phys.* **83**, 2889 (1985).
- ¹⁸ G. M. Jursich and J. R. Wiesenfeld, *Chem. Phys. Lett.* **119**, 511 (1985).
- ¹⁹ J. E. Butler, G. M. Jursich, I. A. Watson, and J. R. Wiesenfeld, *J. Chem. Phys.* **84**, 5365 (1986).
- ²⁰ Y. Huang, Y. Gu, C. Liu, X. Yang, and Y. Tao, *Chem. Phys. Lett.* **127**, 432 (1986).
- ²¹ P. M. Aker and J. J. Sloan, *J. Chem. Phys.* **85**, 142 (1986).
- ²² C. B. Cleveland, G. M. Jursich, M. Trolrier, and J. R. Wiesenfeld, *J. Chem. Phys.* **86**, 3253 (1987).
- ²³ J. J. Sloan, *J. Phys. Chem.* **92**, 18 (1988).
- ²⁴ T. J. Sears, G. E. Hall, and J. J. F. McAndrew, *J. Chem. Phys.* **91**, 5201 (1989).
- ²⁵ R. D. Levine, B. R. Johnson, and R. B. Bernstein, *Chem. Phys. Lett.* **19**, 1 (1973).
- ²⁶ R. E. Howard, A. D. McLean, and W. A. Lester, *J. Chem. Phys.* **71**, 2412 (1979).

- ²⁷R. Schinke and W. A. Lester, *J. Chem. Phys.* **72**, 3754 (1980).
- ²⁸J. N. Murrell, S. Carter, I. M. Mills, and M. F. Guest, *Mol. Phys.* **42**, 605 (1981).
- ²⁹P. A. Whitlock, J. T. Muckerman, and E. R. Fisher, *J. Chem. Phys.* **76**, 4468 (1982).
- ³⁰S. W. Ransome and J. S. Wright, *J. Chem. Phys.* **77**, 6346 (1982).
- ³¹L. J. Dunne and J. N. Murrell, *Mol. Phys.* **50**, 635 (1983).
- ³²J. N. Murrell and S. Carter, *J. Phys. Chem.* **88**, 4887 (1984).
- ³³G. Durand and X. Chapuisat, *Chem. Phys.* **96**, 381 (1985).
- ³⁴K. Rynefors, P. A. Elofson, and L. Holmlund, *Chem. Phys.* **100**, 53 (1985).
- ³⁵M. S. Fitzcharles and G. C. Schatz, *J. Phys. Chem.* **90**, 3634 (1986).
- ³⁶J. K. Badenhoop, H. Koizumi, and G. C. Schatz, *J. Chem. Phys.* **91**, 142 (1989).
- ³⁷E. M. Goldfield and J. R. Wiesenfeld, *J. Chem. Phys.* **93**, 1030 (1990).
- ³⁸P. J. Kuntz, B. I. Niefer, and J. J. Sloan, *Chem. Phys.* **151**, 77 (1991).
- ³⁹G. C. Light, *J. Chem. Phys.* **68**, 2831 (1978).
- ⁴⁰A. C. Luntz, *J. Chem. Phys.* **73**, 1143 (1980).
- ⁴¹K. H. Gericke, F. J. Comes, and R. D. Levine, *J. Chem. Phys.* **74**, 6106 (1981).
- ⁴²F. J. Comes, K. H. Gericke, and J. Manz, *J. Chem. Phys.* **75**, 2853 (1981).
- ⁴³H. Okabe, *Photochemistry of Small Molecules* (Wiley-Interscience, New York, 1978).
- ⁴⁴G. Herzberg, *Spectra of Diatomic Molecules* (Van Nostrand-Reinhold, New York, 1950).
- ⁴⁵J. Brzozowski, P. Erman, and M. Lyyra, *Phys. Scr.* **17**, 507 (1978).
- ⁴⁶J. A. Coxon, *Can. J. Phys.* **58**, 933 (1980).
- ⁴⁷G. H. Dieke and H. M. Crosswhite, *J. Quantum Spectr. Radiat. Transfer* **2**, 97 (1962).
- ⁴⁸W. L. Dimpfl, J. K. Kinsey, *J. Quantum. Spectrosc. Radiat. Transfer* **21**, 233 (1979).
- ⁴⁹D. L. Baulch *et al.*, *J. Chem. Ref. Data* **13**, 1259 (1984).
- ⁵⁰R. K. Sparks, L. R. Carlson, K. Shobatake, M. L. Kowalczyk, and Y. T. Lee, *J. Chem. Phys.* **72**, 1401 (1980).
- ⁵¹C. E. Fairchild, E. J. Stone, and G. M. Lawrence, *J. Chem. Phys.* **69**, 3632 (1978).
- ⁵²Bronstein-Semendjajew, *Taschenbuch der Mathematik* (Verlag Harry Deutsch, Frankfurt a. M., 1970).
- ⁵³(a) K. Mikulecky, K.-H. Gericke, and F. J. Comes, *Chem. Phys. Lett.* **182**, 290 (1991); (b) K. Mikulecky, K. H. Gericke, and F. J. Comes, *Ber. Bunsenges. Phys. Chem.* **95**, 927 (1991).
- ⁵⁴P. A. Berg, J. J. Sloan, and P. J. Kuntz, *J. Chem. Phys.* **95**, 8038 (1991).